Design of Partial Discharge Real-Time Capture System

Yu-En Wu

National Kaohsiung University of Science and Technology, Kaohsiung, Taiwan
Email: yew@nkust.edu.tw

Abstract—**This paper presents an online partial discharge real-time capture system whose system architecture includes Field-programmable Gate Array (FPGA) components, a Human–Machine Interface (HMI), and analog amplifying circuits. The analog amplify circuit is designed to achieve a magnification rate of 10 times and a bandwidth of 100 MHz. The software developed in this work can be used for real-time online monitoring, recording, and analysis of partial discharge. The captured signal of the partial discharge was analyzed by the FPGA by using a fast Fourier transform, time–frequency map, and phase-resolved partial discharge, and the results were transmitted through the RS-232 to the HMI for display. System stability is improved through data analysis to determine possible causes of partial discharge, averting both user risk and damage to equipment.**

Index Terms—**Field-programmable gate array, partial discharge, real-time online monitoring**

I. Introduction

Partial Discharge (PD) usually occurs in the insulator or surface electric field concentration area. It produces chemical reactions that damage the insulating material through erosion and causes a discharge effect in the concentrated electric field area. The insulation material deterioration can result in instrument damage and endanger user safety.

Multiple types of voltage power equipment are used to maintain the power supply and deploy the hub in power systems. The power equipment is mainly composed of conductive, magnetic, structural, and insulating materials. When the insulation material is exposed to high voltage because of internal defects, poor construction, or external environmental factors caused by PD, the life of the equipment often depends on the insulation strength of the insulation material. The longer the equipment is used, the more serious the deterioration, which can lead to accidents [1]-[5].

Per expert experiential statistics, 60%–80% of accidents are caused by insulation failure and aging in power equipment operation. Therefore, if detection technology can be used to detect the insulation status of the equipment and for further analysis and research to diagnose and prevent faults, equipment failure rates can be reduced and equipment life considerably improved [6].

In general, employing offline PD detection technology when the equipment stops operating is impractical. To address this drawback, this paper presents a PD detection system with online monitoring, recording, and analysis functions as well as a variety of analytical tools to detect PD signals for more accurate judgments.

II. Literature Review

A. Causes and Effects of PD

PD can be defined as a localized electrical discharge that partially bridges the insulation between conductors [7]. It may appear in gaps or cracks in solid insulation material, in liquid insulation bubbles, or in the metal surface or other parts of the tip. This discharge effect reduces the insulation strength, gradually leading to complete insulation failure. When the insulation material is defective, the electrical equipment can intermittently malfunction, which causes the equipment to become damaged or even may explode, endangering users.

PD can be roughly divided into three types: corona discharge, surface discharge, and internal discharge. Corona discharge refers to the discharge phenomenon of gas as a medium. Surface discharge refers to the discharge phenomenon that occurs on the surface of the insulating material, and internal discharge is the recapitulation of the discharge inside the insulating material [8]. These are detailed separately, as follows.

1) Internal discharge

Insulation material may contain cracks, impurities, air gaps, or similar defects, concentrating the local electric field and resulting in defects where the electric field strength is greater, in turn producing discharge. In the long term, the discharge may lead to insulation defects comparable with those caused by destroyed insulation, with the discharge situation depending on the characteristics of the insulating material. The discharge pulse usually occurs in the first or third quadrants [8].

2) Surface discharge

Because of the air gap between the insulating material and the conductor, the charge can only accumulate on the insulating material. The relationship between the electric field and the charge decay causes the discharge to mostly occur in the first or third quadrant. In addition, because of the asymmetry of the electrode, during the negative half-cycle, the free electrons resulting from the secondary electron emission caused by the impact of positive charges on the cathode could trigger new discharge [9].

3) Corona discharge

Corona discharge is a gas ionization phenomenon caused by the local discharge stress of the insulation system exceeding the critical value. The main reason for corona occurrence is that the conductor presents a tip, such that the tip of the protrusion is too high near a strong electric field, resulting in air ionization generating the corona discharge phenomenon. High-voltage power equipment often experiences corona discharge due to the design, manufacture, and improper installation [8].

B. PD Detection Method

On the basis of the type of PD signal, PD sensing methods can be sorted into three main categories, which is described as follows [10].

1) Electrical detection

Ultrahigh frequency (UHF) sensors or UHF antennas can detect electromagnetic waves generated by PD (frequency range: 300 MHz to 3 GHz). UHF sensors are typically used to detect PD in gas insulation systems and transformers, and they shield external noise and disturbances effectively. Thus, UHF sensors for PD signals have attracted increasing attention. However, transformers with different internal geometries have different impedances, and UHF sensors must be recalibrated to accommodate this.

High frequency current transformer (HFCT) sensors detect the high frequency current pulse generated by PD. The frequency band of an HFCT sensor is usually from several hundred kilohertz to several tens of megahertz. It has been proven capable of capturing partial discharge signals. HFCT sensors are composed of a magnetic core and shielded windings. With a measurement clamp around the case ground of the components, HFCT sensors with split cores can easily be applied to measure the current pulse of high-voltage equipment without disconnecting any part of it.

2) Acoustic detection

Acoustic sensors can be used to detect acoustic and ultrasonic waves generated by PD. Acoustic sensors are usually used to detect PD in switchgear, gas insulated systems, and transformers. Using acoustic sensors to detect a partial discharge signal has several advantages. First, they are easy to install; for example, sensors can be installed outside of a transformer wall while the transformer remains in full service. Second, the acoustic sensor is immune to electromagnetic interference. Third, acoustic sensors are low cost and perform well for localizing the PD sources. However, acoustic sensors have some limitations, such as low sensitivity if the background noise is serious.

3) Chemical detection

Chemical detection of PD involves detecting the products of chemical reactions caused by discharge. Dissolved gas analysis (DGA) is the main type of chemical detection, and it focuses on analyzing the dissolved gases in the transformer oil. DGA methods include gas chromatography and online hydrogen monitoring. The distribution of collected gases can assist in identifying the type of PD. However, chemical detection is typically an intrusive detection method, which limits its scope of application. Moreover, chemical detection cannot provide any information about the PD location.

C. PD Analysis Method

1) Phase-resolved partial discharge

In [11], phase-resolved partial discharge (PRPD) assisted in analyzing the types of defect, such as corona discharge, surface discharge, or internal discharge. The PRPD shows the supply mains phase and the discharge voltage of the PD. Depending on the type of defect, the PRPD has different discharge characteristic clusters, which help to differentiate them.

2) Time–frequency ma

Time-frequency (T-F) map theory leverages the property that partial discharge pulses and noise pulses have different shapes. Therefore, the recorded waveforms are assigned to different clusters based on the equivalent time and frequency [12].

The various types of pulses discussed in [12] have different waveform characteristics, depending on the partial discharge properties generated by the insulation defects as well as transfer functions that discharge pulses from the discharge source to the coupling device. In addition, the partial discharge pulse waveform shapes are different from most interference pulses.

To distinguish the acquired pulse waveforms considering the time and frequency centers of each signal, the average time and the average frequency were used. Expressed in this manner, different pulse shapes can be distinguished and displayed in different clusters of the T-F map.

D. Laboratory Setup for PD Signal Measurement

To facilitate the measurement of signals in the experiments, we set up the high-voltage PD simulation platform shown in Fig. 1. Using the auto-transformer to adjust the voltage, the high-voltage converter amplified the output voltage 200 times and was then connected to the defective insulation material. Finally, an HFCT was implemented to measure the PD current.

Fig. 1. High-voltage PD simulation platform.

III. SYSTEM HARDWARE AND SOFTWARE STRUCTURE

A. System Processes

Fig. 2 displays the structure of the proposed system's processes. BNC (Bayonet Neill–Concelman) input supplies the HFCT-induced voltage, which is amplified tenfold by the preamplifier because the discharge signals generated by the power equipment are otherwise too small. Then, the ADC converts this voltage to an 8-bit digital value, which is sent to the Field-Programmable

Gate Array (FPGA) for analysis by differential signalling. The FPGA obtains the Human–Machine Interface (HMI) settings by RS232 and processes data based on the HMI settings in the Wave Data Process. The PRPD Process performs frequency detection, zero crossing detection, and phase counting, as well as processing the divide clock; it then transfers the results of the Wave Data Process and PRPD Process to the NIOS, which are respectively processed by the fast Fourier transform (FFT) and T-F map analysis. Per the HMI settings, the results of the analysis are transmitted by the RS-232 to the HMI.
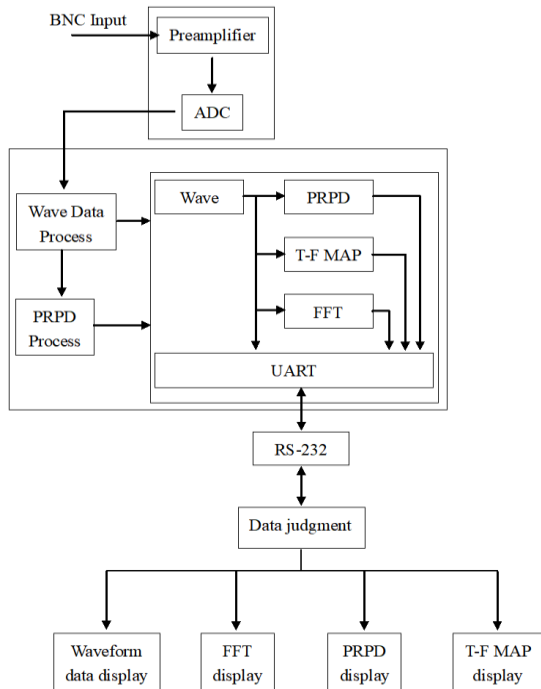
Fig. 2. System processes.
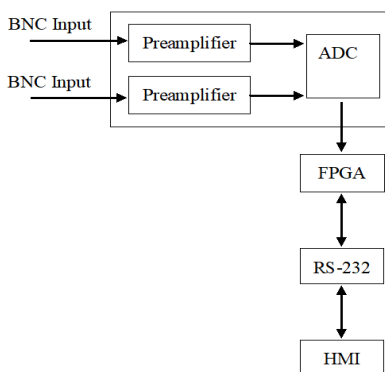
Fig. 3. Hardware structure.
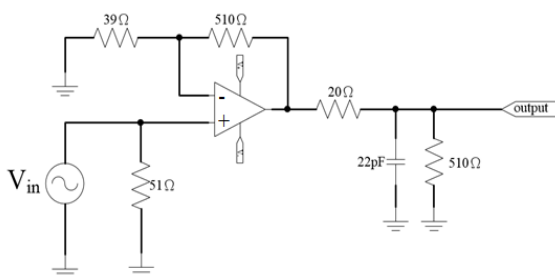
Fig. 4. Preamplifier design.
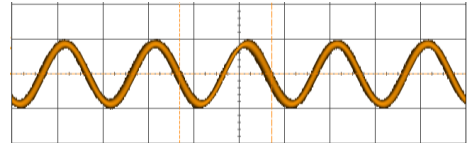
(Voltage: 500 mV/div; time: 500 ns/div)

Fig. 5. Output waveform (1 MHz).
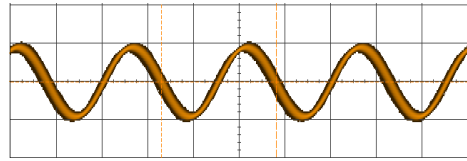
(Voltage: 500 mV/div; time: 10 ns/div)

Fig. 6. Output waveform (40 MHz)
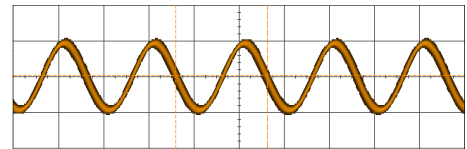
(Voltage: 500 mV/div; time: 5 ns/div)

Fig. 7. Output Waveform (100 MHz).

B. Hardware Structure

Fig. 3 illustrates the hardware structure of the proposed system. Note that it has two input channels. However, the power equipment of the insulation deterioration generate to discharge signals are too small, the preamplifier to magnify the signal 10 times before the signal conversion. After using ADC to convert the voltage to 8 bits digital value, and then transmission to the FPGA board for signal analysis by differential signalling. When the signal analysis is completed, through the RS232 to send analysis results to the human machine interface (HMI), as shown in Fig. 3, the analysis results will be presented graphically.

The FPGA suite as purchased supports three magnification levels ($2\times$, $3.5\times$, and $8.5\times$) and a test frequency up to 5 MHz. However, the high-voltage PD simulation platform output voltage is too low and the frequency may reach 100 MHz; therefore, a preamplifier was designed to replace the preamplifier on FPGA suite to support a bandwidth of 100 MHz and 10 times magnification (Fig. 4).

To verify the operation of the preamplifier, the waveform was tested at 1 MHz, 40 MHz, and 100 MHz. With a sine wave whose peak to peak value is 100 mV as the input, the outputs are shown in Fig. 5 to Fig. 7.

C. Software Structure

1) HMI software planning

When the program is loaded, the settings are initialized and users can set the trigger mode and analysis function per their usage requirements. The analysis data sent by the FPGA to the HMI, and the manner in which the data are displayed, are based on the HMI settings (Fig. 8).

2) FPGA internal planning

The internal architecture of the FPGA is shown in Fig. 9. CLK1 and CLK2 are 125 MHz and 50 MHz, respectively. The ADC output value (ADC_Out) is sent to the double data rate I/O (DDIO), and the two sets of channel

data are separated. The data is subsequently sent to the memory controller, which performs preliminary data processing according to the HMI settings before saving the data into RAM. CLK2 proceeds through the phase-locked loop (PLL), where its frequency is raised to 60 MHz as the NIOS working clock. In the CLK divider and detection grid frequency, the CLK2 frequency is decreased to 50 Hz and then raised to 2.7 kHz; this is used to calculate the frequency of the grid. In the detect the zero crossings and degree counter, the 50 Hz generated by the CLK Divider And Detection Grid Frequency is used to calculate the grid phase, and then zero crossing detection is used to judge whether the current phase of the grid is greater than 180°. The calculation results are then sent to NIOS for the final data analysis. Finally, using the universal asynchronous receiver/transmitter (UART) as a communication interface, the data is sent to HMI through the RS232.
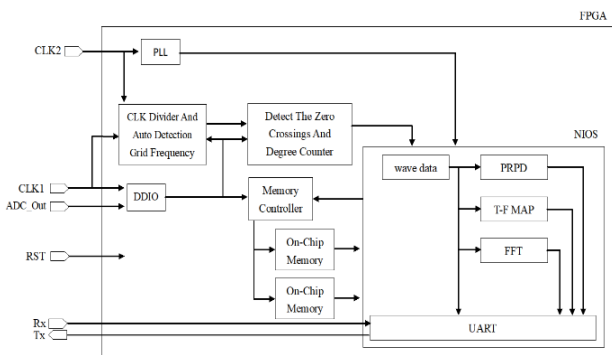

Fig. 8. FPGA internal planning.

Fig. 9. FPGA internal architecture.

IV. System Test

The partial discharge signal acquisition system proposed in this paper can be divided into three parts: FPGA peripheral hardware, program design, and HMI programming. With the FPGA as the system core, a variety of analyses can be performed on externally input
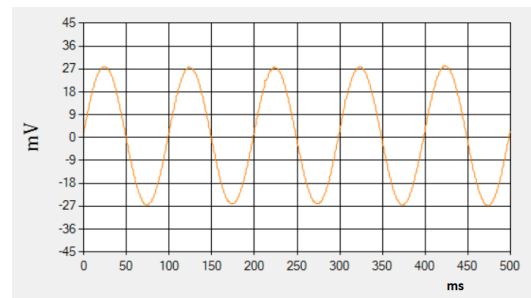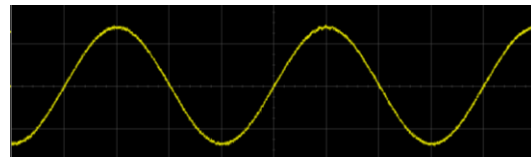
information, and after a series of operations, the results of the analysis can be output through the RS-232 communication interface to the HMI, which then displays the analysis results (Fig. 10).

Fig. 10. HMI.

Fig. 11. HMI waveform display test (1.25MHz).

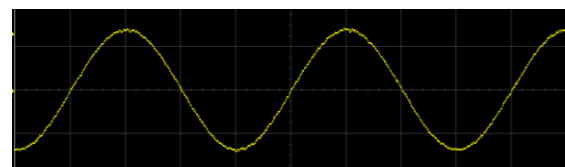(Voltage: 20 mV/div; time: 200ns/div)
Fig. 12. Input waveform (1.25MHz).

A. Waveform Display

This system function detects a PD signal in the absence of any analysis. Fig. 11 displays the waveform display test on the HMI and Fig. 12 shows the input test waveform (a 1.25 MHz sine wave).

B. Fast Fourier Transform

The partial discharge signal detected by the system is subjected to FFT, which can analyze the frequency of the partial discharge signal. To verify the FFT, the signal generator was used to produce a 5 MHz sine wave (Fig. 13 and Fig. 14). The six graphs indicate that the FFT analysis result is exactly the same as the frequency of the signal generator, which proves that the FFT of the system is extremely accurate.

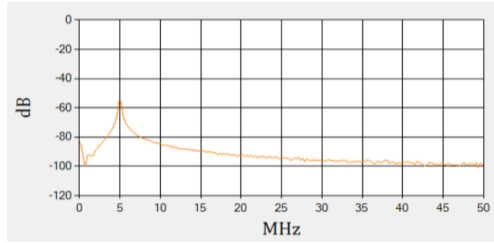(Voltage: 20 mV/div; Time: 50 ns/div)
Fig. 13. Input waveform (5MHz).

Fig. 14. FFT analysis result (5 MHz).

C. Phase-Resolved Partial Discharge

To verify the correctness of the phase, the system input pulse was compared against an oscilloscope in four quadrant pulse wave phases. The results are shown in Fig. 15 to Fig. 22. In Fig. 15 and Fig. 16, the angles were respectively 53.7° and 53°; in Fig. 17 and Fig. 18, they were 109.7° and 110°; in Fig. 19 and Fig. 20, they were 243.4° and 244°; and in Fig. 21 and Fig. 22, they were 351.4° and 350°. The error never exceeds 2°, which confirms that the PRPD phase of the system is extremely accurate.
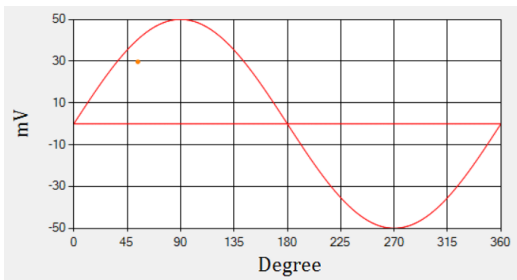
Fig. 15. PRPD analysis result (first quadrant).
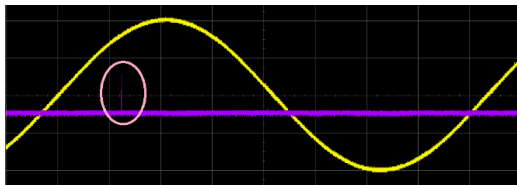
(Voltage: 500 mV/div; Time: 2 ms/div)

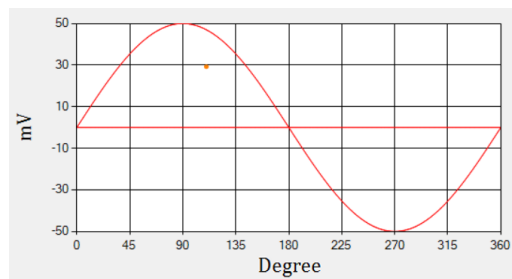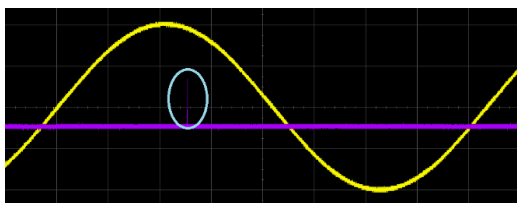Fig. 16. Input waveform (first quadrant).

Fig. 17. PRPD analysis result (second quadrant).

(Voltage: 500 mV/div; time: 2 ms/div)

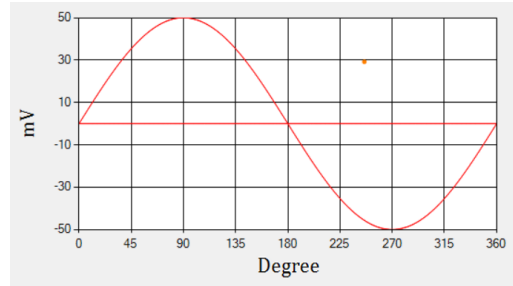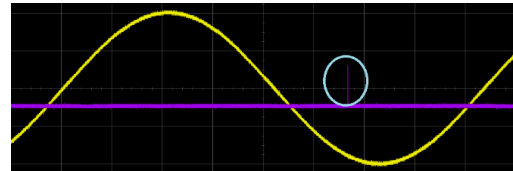Fig. 18. Input waveform (second quadrant).

Fig. 19. PRPD analysis result (third quadrant).

(Voltage: 500 mV/div; time: 2 ms/div)

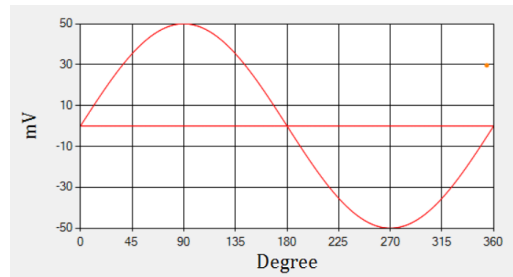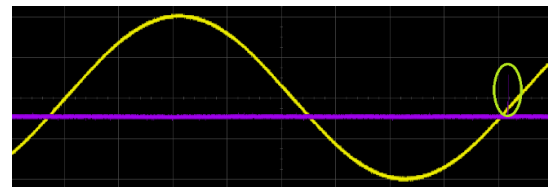Fig. 20. Input waveform (third quadrant).

Fig. 21. PRPD analysis result (fourth quadrant).

(Voltage: 500 mV/div; time: 2 ms/div)
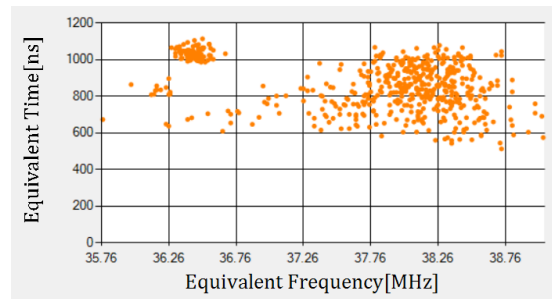
Fig. 22. Input waveform (fourth quadrant).

Fig. 23. T–F MAP analysis result.

D. T–F Map

Using the original partial discharge signal and the FFT analysis results, the equivalent time and the equivalent frequency can be calculated to obtain a clearer signal composition image (Fig. 23).

E. Archived Data

Two types of archiving methods exist in the HMI. The waveform archive stores only the original partial discharge signal, and the two data channels are stored at

the same time. The Y-axis represents the FPGA output numerical data after conversion and storage; Fig. 24 (a) shows the archived results. The feature archive saves the results of the FFT, PRP, and T–F maps, so that data for only one channel is stored. The X-axis, Y-axis, and FPGA output numerical data are converted and then stored; Fig. 24 (b) to Fig. 24 (d) display some archived results.
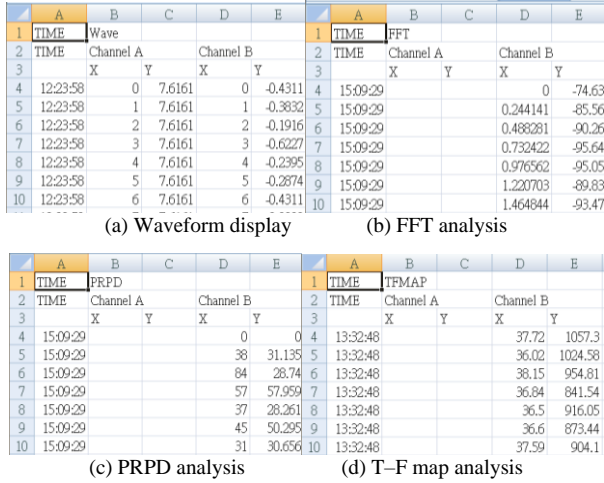

(a) Waveform display   (b) FFT analysis

(c) PRPD analysis   (d) T–F map analysis

Fig. 24. Archived data.
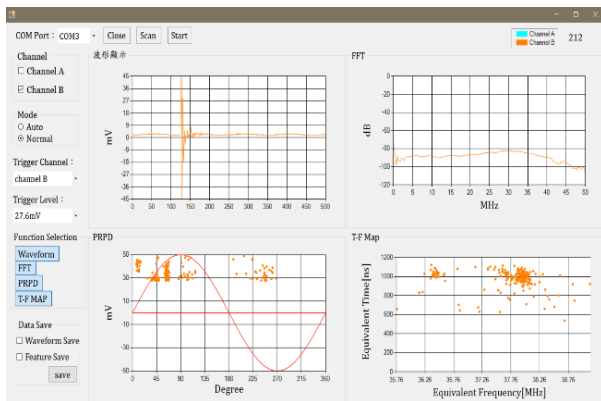

Fig. 25. FPGA entity.

Fig. 26. Actual PD test analysis.

V. Experimental Results

The core system of the FPGA (Fig. 25) can automatically detect the external input of the mains frequency and the data for a variety of analyses, and then (depending the HMI settings) send the analysis results to the HMI to be displayed graphically (Fig. 26).The upper left side of the figure displays the partial discharge signal; the upper right the FFT analysis, according to which the local discharge signal frequency falls between 30–35 MHz; and the lower left is the PRPD analysis. The figure indicates that most of the partial discharge occurs in the first and third quadrants. In addition, the computer interface is capable of providing data archiving functions for different data archiving needs, whether waveform archiving to store the waveform display information, or feature archives to store FFT, PRPD, or T-F map analysis data.

VI. Conclusion

This paper presents a partial discharge real-time capture system, whose structure includes an FPGA suit and preamplifier, which can achieve online monitoring, recording, and analysis functions using the HMI presented in this paper. The system's chief advantages are as follows.

1) This invention can monitor, record, and analyze partial discharge while the system is online, making it practical for ensuring user safety.
2) It can accurately capture the PD signal generated by equipment or underground cables.
3) Its data analysis capability enables observing whether the insulation of the power equipment is safe, and the causes of partial discharge may be determined based on the measured results.
4) It is small, lightweight, and easy to carry.

Conflict of Interest

The author declare no conflict of interest.

References

[1] J. J. Zeng, "Implementation of a dispersed partial discharge monitoring module," Master thesis, National Taiwan University of Science and Technology, July 2011.

[2] Partial Discharge Measurements. [Online]. Acailable: https://electrical-engineering-portal.com/download-center/books-and-guides/power-substations/transformer-testing

[3] V. Vahidinasab, A. Mosallanejad, and A. Gholami, "Partial discharge theory, modeling and applications to electrical machines," in *Proc. 5th Int. Conf. on Electric Power Systems, High Voltages, Electric Machines*, Tenerife, Spain, 2005, pp. 130-135.

[4] Partial Discharge Measurement. [Online]. Acailable: http://www.phenixtech.com/Files/Admin/technicalpapers/Partial%20Discharge%20Measurements.pdf

[5] V. Warren, G. Stone, and H. Sedding, "Partial discharge testing – a progress report," presented at Iris Rotating Machine Conference, June 21, 2017.

[6] C. C. Kuo, "Study on GIS partial discharge," St. John's University, Jan. 1998.

[7] M. Azharudin, M. Isa, M. R. Adzman, *et al.*, "Techniques on partial discharge detection and location determination in power transformer," in *Proc. Int. Conf. on Electronic Design (ICED)*, Aug. 2016, pp. 537-542.

[8] J. T. Chang, "Insulation status assessment of cable terminator based on digital partial discharge measurement," master thesis, National Taiwan University of Science and Technology, July 2005.

[9] C. Pan, K. Wu, Y. Du, *et al.*, "The effect of surface charge decay on the variation of partial discharge location," *IEEE Trans. on Dielectrics and Electrical Insulation*, vol. 23, no. 4, pp. 2241-2249, Aug. 2016.

[10] M. Wu, H. Cao, J. Cao, *et al*., "An overview of state-of-the-art partial discharge analysis techniques for condition monitoring," *IEEE Electrical Insulation Magazine*, vol. 31, no. 6, pp. 25-35, Oct. 2015.

[11] D. Götz, F. Petzold, H. Putter, *et al*., "Localized PRPD pattern for defect recognition on MV and HV cables," presented at Transmission and Distribution Conference and Exposition (T&D), May 2016.

[12] G. C. Montanari, F. Ciani, and A. Contin, "Accelerated aging, partial discharges and breakdown of Type II turn-to-turn insulation system of rotating machines," in *Proc. IEEE Electrical Insulation Conference (EIC)*, 2016, pp. 190-193.

Yu-En Wu was born in Chia-Yi, Taiwan, in 1964. He received the B.S. degree in electrical engineering from Taiwan Institute of Technology, Taipei, Taiwan, in 1989, the M.S. degree in electrical engineering from Sun Yat-Sen University, Kaohsiung, Taiwan, in 1992, and the Ph.D. degree in electrical engineering from National Chung Cheng University, Chia-Yi, Taiwan, in 2005. From 1992 to 2005, he was a Lecturer in the Department of Electronic Engineering, Wu Feng Institute of Technology, Chia-Yi, Taiwan. He was an associate professor at the same institute. He is currently a professor at Department of Electronic Engineering, National Kaohsiung University of Science and Technology. His research interests include Bidirectional DC/DC converter and implementation of multi-inverter systems, Power Electronics, DSP based application systems, Smart grid and Renewable energy systems.